University of Tehran Press

Pollution

Print ISSN: 2383-451X
Online ISSN: 2383-4501

https://jpoll.ut.ac.ir/

Effective Removal of Indigo Carmine in Aqueous Solutions using a Low-Cost Adsorbent Developed from Corn Husk Waste: Synthesis, Batch, and Optimization Studies

Tuti Handayani[1,2] | Emriadi[1] | Deswati[1] | Putri Ramadhani[1] | Rahmiana Zein[1]✉

1. Department of Chemistry, Faculty of Mathematics and Natural Sciences, Andalas University, PO Box 25163 Padang, Indonesia.
2. Department of Pharmacy, Fort De Kock University, PO Box 26117 Bukittinggi, Indonesia.

Article Info

Article type:
Research Article

Article history:
Received: 2 March 2023
Revised: 14 May 2023
Accepted: 23 Jun 2023

Keywords:
Adsorption
Corn husk
Indigo carmine
Low-cost
Waste

ABSTRACT

Acid-activated corn husk waste (CHW) was used to investigate the adsorption mechanism of Indigo Carmine (IC) dye from an aqueous solution. The effect of different operating parameters such as pH (1-7), initial IC dye concentration (40-400 mg/L), contact time (5-75 min), and heating temperature (25–200 °C) was measured on the removal of IC dye by the CHW. The maximum uptake of IC dye was observed at an initial pH of 2. The maximum capacity of 13.57 mg/g and the maximum dye removal of 89.01 % in wastewater. The adsorbents were characterized using Fourier Transforms Infrared Spectrophotometry (FTIR), Scanning Electron Microscopy (SEM), Brunauer-Emmett-Teller (BET) surface area analysis, X-ray Fluorescence (XRF), and Thermogravimetry Analysis. The characterization process reveals the differences in adsorbent characteristics before and after the adsorption processes. The Langmuir showed the best fitting (R2 = 0.977) and described multilayer adsorption on diverse surfaces. The pseudo-second-order kinetic model best correlated with the experimental data (R2 = 0.981). Thermodynamics revealed that adsorption was favorable spontaneous and exotherm. The study's results indicated that using CHW as a low-cost adsorbent to treat IC dye was efficient and beneficial to the environment.

Cite this article: Handayani, T., Emriadi, Deswati, Ramadhani, P., & Zein, R. (2023). Effective Removal of Indigo Carmine in Aqueous Solutions using a Low-Cost Adsorbent Developed from Corn Husk Waste: Synthesis, Batch, and Optimization Studies. *Pollution*, 9 (4), 1396-1413.
https://doi.org/10.22059/POLL.2023.355474.1813

 Publisher: University of Tehran Press.
DOI: https://doi.org/10.22059/POLL.2023.355474.1813

INTRODUCTION

A significant environmental worry is increased water contamination by humans, technical advancements, and the quickening of industry expansion. Synthetic dyes and chemicals in the industry produce large amounts of contaminated water (Islam et al., 2021). The dye residue disturbs the natural processes of receiving water by blocking the light needed for photosynthesis and leaving an unsightly aesthetic impression. In addition, these dyes can be accumulated in aquatic animals and, consequently, get into the alimentary chain and reach human beings (Bazan & Robert, 2023; Lakshmi et al., 2009). According to the World Health Organization and the United Nations Educational, Scientific, and Cultural Organization standards, toxic dyes are a major public concern; indigo carmine at a concentration above 0.005 mg/L is unacceptable in water. This has led to the development of effective treatment solutions for wastewater-containing dyes.

Adsorption was a popular procedure that is frequently used to remove the dye. Adsorbents

*Corresponding Author Email: *mimiedison@yahoo.co.id*
rzein@sci.unand.ac.id

for dye degradation could be essential tools for wastewater treatment (Hwa et al., 2022). Several biosorbents have been reported, such as adsorption of Rhodamine B by Raspberry seed nanocarbon and Wheat flour (Bazan & Robert, 2023; Hasan et al., 2021), removal of Methylene blue by Turmeric powder, Lemongrass biowaste (Kubra etal., 2021; Zein et al., 2022), removal of methyl orange by rice flour and graham flour (Md. Munjur et al., 2020), removal of Congo Red dye from Industrial wastewater using *Teucrium polium L* (Alamrani & Al-Aoh, 2021), removal of crystal violet by graham flour (Kubra et al., 2021), and use of Cinnamon bark (Güler et al., 2021) *Terminalia catappa* shells (Hevira et al., 2020), and activated Pomegranate peel (Abbas et al., 2022) to adsorb IC. The utilization of organic materials as biosorbents show excellent capability for the removal of dye.

Corn husk is an agricultural waste obtained from the cornfield after harvest. It was inexpensive and widely available. Corn husk has good adsorptive properties and has been used for the removal of various dyes (Malik et al., 2016; Paşka et al., 2014; Ponce et al., 2021), heavy metals (Paul et al., 2016; Sanka et al., 2020; Shan et al., 2013), and other compounds like phenol (Mishra et al., 2019; Sengupta & Balomajumder, 2014). The present study was intended to examine and explore the removal of IC dye using CHW. Based on the literature that has been read, there has never been a study on IC dye adsorption using CHW. **T**he study was new research for utilizing the corn husk waste activated using acid (HNO3) as a low-cost biosorbent. The effects of adsorption parameters like pH, initial concentration, contact time, and heating temperature have been investigated. The equilibrium isotherm model with error functions, kinetic rate models, and thermodynamic parameters was also evaluated, presented, and discussed to predict and evaluate the adsorption mechanism.

MATERIAL AND METHODS

The process for making CHW is that the samples of corn husk were collected in Sangkir Lubuk Basung West Sumatera. The corn husk was washed with distilled water to remove impurities. After washing, it dried at room temperature for 1-2 weeks. The dried samples were ground and homogenized at ≤36 µm. Then an acid treatment was carried out by placing the corn husk powder in a 0.01M HNO_3 solution for 120 minutes (Hevira et al., 2020), filtering, washing until neutral, and drying at 60 °C for 60 minutes (Amer et al., 2017).

The biosorption investigations were carried out using the batch methodology. Several parameters were investigated, pH (1–7) was adjusted by a pH buffer, initial dye concentration (40-400 mg/L), contact time (5–75 min), and heating temperature (25–200 °C by using spectrophotometry UV-vis (Shimadzu 1240) at a maximum absorbance wavelength of 609 nm while the sample solution was stirred at 100 rpm. Equations (1) and (2) were used to determine the equilibrium biosorption capacity of acid CHW for IC dye removal and removal efficiency (%R)(Yeo et al., 2023; Yous et al., 2019).

$$q = \frac{(C_0 - C_e)}{m} \, x \, V \tag{1}$$

$$\%R = \frac{(Co - Ce)}{Co} \, x \, 100 \tag{2}$$

Where the mass of CHW is m (g), the initial IC dye concentration is C_0 (mg/L), the final IC dye concentration is Ce (mg/L), and the volume of the IC dye solution is V (L).

The adsorption isotherm study was used to decide on the relevant isotherm model, which was an R^2 value close to 1 (Ramesh et al., 2013). The experimental data from the initial concentration parameter was analyzed to investigate the adsorption isotherm study of the Langmuir, Freundlich, Temkin, and Dubinin-Radushkevic models. The linearised form of the models was described in Equations 3-6, respectively.

$$\frac{C_e}{qe} = \frac{1}{K_L qm} + \frac{C_e}{qm} \quad (3)$$

$$\log qe = \log k_F + \frac{1}{n} \log C_e \quad (4)$$

$$qe = \beta \ln K_T + \beta \ln C_e \quad (5)$$

$$\ln qe = \ln qm - k_{DR}\, \varepsilon^2 \quad (6)$$

$$\varepsilon = RT\ln\left(1 + \frac{1}{C_e}\right)$$

$$E_{DR} = (2K_{DR})^{-0.5}$$

Based on the separation factor value (R_L), analysis of the Langmuir isotherm model may also help to determine whether the adsorption procedure is feasible (Ahmad & Ansari, 2020). Adsorption was irreversible and beneficial when RL = 0 and 0 < RL <1. Equation 7 can be employed to get the R_L value. Adsorption was unfavorable when 0 < R_L <1 and irreversible when R_L = 0 (Ramadhani et al., 2021).

$$R_L = \frac{1}{1 + K_L C_0} \quad (7)$$

The time-dependent adsorption capacity was analyzed using adsorption kinetics. An adsorption kinetics model was developed using contact time. The adsorption mechanism and rate-limiting phase were discovered by studying the kinetic models, Pseudo-first-order (Equation 8) (Hoang et al., 2021), Pseudo-second-order (Equation 9) (Lagergren, 1898; Purnaningtyas et al., 2020), Intraparticle diffusion (Equation 10) (Al-Abbad & Alakhras, 2020), Elovich (Equation 11) (Abbas et al., 2022). Applying a kinetic model occurs when R^2 approaches 1 (Chandra et al., 2019).

$$\ln(qe - qt) = \ln qe - k_1 t \quad (8)$$

$$\frac{t}{qt} = \frac{1}{k_2 qe^2} + \frac{1}{qe} t \quad (9)$$

$$qt = k_{Diff} t^{0.5} + C \quad (10)$$

$$qt = \left(\frac{1}{\beta}\right) \ln(\alpha\beta) + \left(\frac{1}{\beta}\right) \ln t \quad (11)$$

RESULT AND DISCUSSION

FTIR was used to predict the functional groups involved in adsorption by analyzing the shift of the FTIR spectrum between 500 and 4000 cm^{-1}. Figure 1 shows that the CHW contains several different types of functional groupings. From the FTIR spectrum, there are O-H functional groups in lignocellulosic (Cellulose, hemicellulose, and lignin), appearing at a wave number of 3406 cm^{-1} was a hydroxyl group, C=C aromatic at 1639 cm^{-1}. The peak at 1031 cm^{-1} indicates the presence of Si-O. In the spectrum, there is no significant shift in wave number before and after contact with IC dye, and there is cellulose, hemicellulose, and lignin in CHW.

SEM coupled with EDX was used to assess the morphological and surface characteristics of acid-activated CHW before and after IC dye removal. The SEM micrographs of the CHW are given in Figure 2. The pores of varying sizes on the surface of CHW are sufficiently big for IC

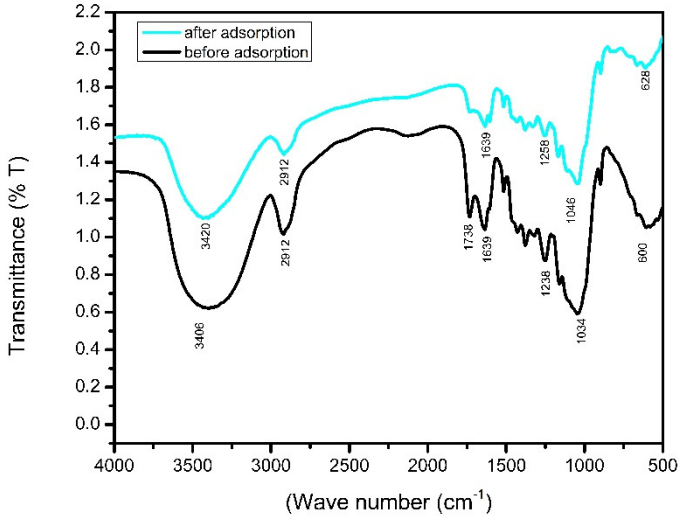

Fig. 1. FTIR spectra of CHW before and after IC dye adsorption

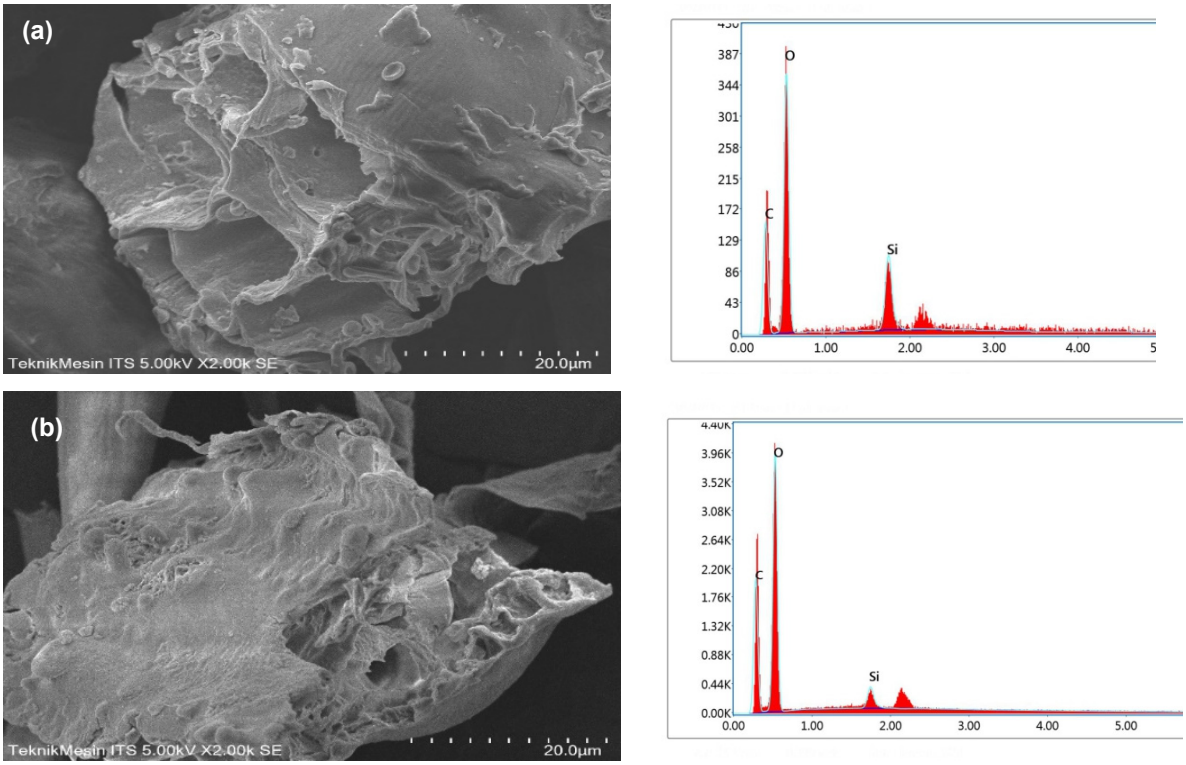

Fig. 2. SEM-EDX of CHW before adsorption (a) and after adsorption (b) of indigo carmine dye (magnifications: 2000x)

dye molecules to entangle and interact with the surface groups of Figure 2(a). In Figure 2(b), an SEM micrograph of IC dye-loaded CHW shows that the surface of the CHW becomes coated due to the molecules of IC dye entering the pores and structure of the cellulose. This porous structure's closure indicates the adsorption given by the diffusion of the IC dye molecules that comprise the packed microstructure onto an appropriate surface. This phenomenon was proven by EDX results (Figure 2 (b)), where the percentage of oxygen atoms increased after the IC dye

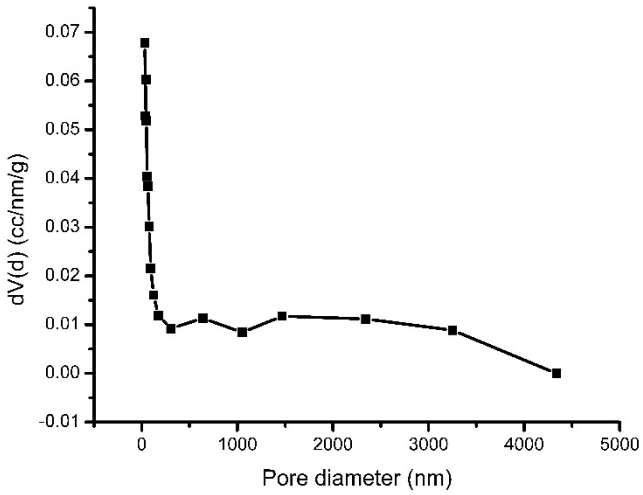

Fig. 3. The pore size distribution of CHW

Table 1. Physicochemical composition of CHW.

Parameter	%
Cellulose	46.40 ± 0.12
Hemicellulose	23.69 ± 0.12
Lignin	11.70 ± 0.12
Moisture	11.15 ± 0.01
Ash	2.08 ± 0.01
Lipid/Fat	6.05 ± 0.09
Protein	1.18 ± 0.06
Extractives	3.91

adsorption processes. They were also found in other biomass such as *Terminalia catappa* shells (Hevira et al., 2020), *Pistia stratiotes* dry (Ferreira et al., 2019), and rice husk ash (Lakshmi et al., 2009) after adsorbing IC dye.

BET was used to measure the surface area of solid or porous materials. The surface area of CHW before biosorption was 15.763 m^2/g, and after biosorption of IC dye was 12.645 m^2/g. It suggests that the surface area of the CHW has electrostatic interaction and contains active sites responsible for the removal of IC dye from an aqueous solution (Hevira et al., 2020)**.** The total pore volume before the removal of IC dye was 0.0442 cm^3/g, and after the removal of IC reduced to 0.0312 cm^3/g. This reduction is related to IC dye's occupation of adsorbent pores (Ferreira et al., 2019). The pore size distribution of the CHW biosorbent was determined using the Barrett–Joyner–Halenda (BJH) method, as shown in Figure 3.

The chemical composition of the adsorbents significantly affects the adsorption capacity, as they are made up of several natural fiber polymers. Determining chemical composition used gravimetric, Kendal, and soxhlet extraction methods. The main compounds of CHW are cellulose, hemicellulose, and lignin, as seen in Table 1. Other constituents are present in small amounts, such as fat, ash, extractives, and protein.

XRF was used to investigate the composition of the inorganic compounds of CHW. Due to the exchange interaction between the IC dye and the cationic molecule or the change in composition following the biosorption of IC dye, the ratio of specific oxides changed. According to the data in Table 2, there was an increase in S after the biosorbent was exposed to IC dye. This finding suggests that IC dye containing S has been associated with CHW.

Table 2. Chemical element analysis (XRF) of CHW before and after IC dye biosorption

Oxide	Before adsorption (%)	After adsorption (%)
SiO_2	69.387	60.568
P_2O_5	15.737	15.296
K_2O	4.226	0.535
S	-	12.118

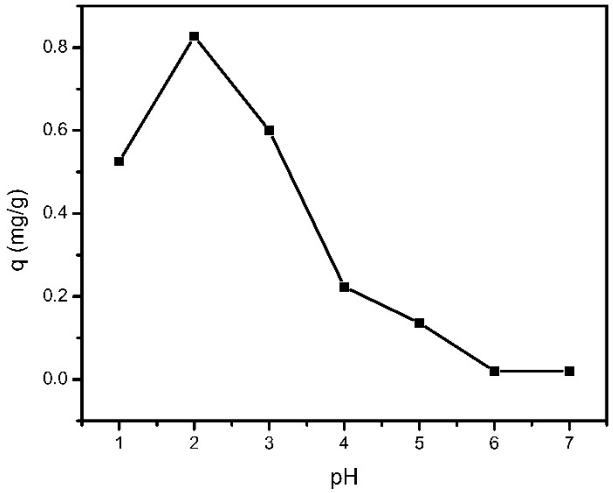

Fig. 4. Effect of pH on IC dye adsorption by ACWH (C_0: 10 mg/L; T = 25°C; V = 10 mL; m = 0,1 g; agitation speed= 100 rpm; t = 60 minutes; and particle size= 36μm).

The optimum condition in the removal operation is determined, such as pH, initial dye concentrations, contact time, and temperature. The pH of the solution was one of the most crucial elements in dye removal. Because hydrogen and hydroxyl ions were present in the solution, the degree of acidity substantially impacted adsorption. As the biosorbent's active site is positively charged and is more robust when H^+ ions are added, Figure 4 illustrates how pH affects the adsorption of negatively charged indigo carmine. Regarding the IC dye adsorption by the *Terminalia catappa* shell, there is less competition for the OH^- and indigo carmine ions, which bind to the adsorbent (Hevira et al., 2020)

The pH_{pzc} CHW was 5.01 following the most recent biosorbent pH_{pzc} measurement. Therefore, below this pH, the biosorbent will be negatively charged and capable of adsorbing IC dye. If the pH is lower than pH_{pzc}, the biosorbent will be positively charged and more capable of adsorbing anionic dyes. The interaction of IC (anionic dye) ions and H^+ on the active site of the biosorbent will aid in the adsorption process, as shown in Figure 4 when the pH is between 1-4 and protonation occurs. As the pH drops, more H^+ ions are in the solution (Hevira et al., 2020). The presence of CHW sites that could bind to IC dyes led to increased biosorption capacity peaked at pH 2.01. Another study on IC dye adsorption on Rice husk (Lakshmi et al., 2009), Cinnamon bark (Güler et al., 2021) was conducted at a pH lower than the pH_{pzc} of the biosorbent. Another study used other anionic dyes, such as reactive red 120 and methyl orange, where the maximum adsorption capacity by activated carbon prepared from Mahagoni Bark occurred at pH 3 (Ghosh et al., 2020; Chakraborty et al., 2021), and the highest percent removal of congo red by *Nymphaea alba* occurred at pH 2 (Rahman et al., 2021).

Adsorbate diffuses from the majority of the liquid phase through the liquid-solid layer into the pores of the adsorbent and towards its active site during the time-consuming mass transfer process known as biosorption. Obtaining the maximal capacity of the biosorbent in adsorbing

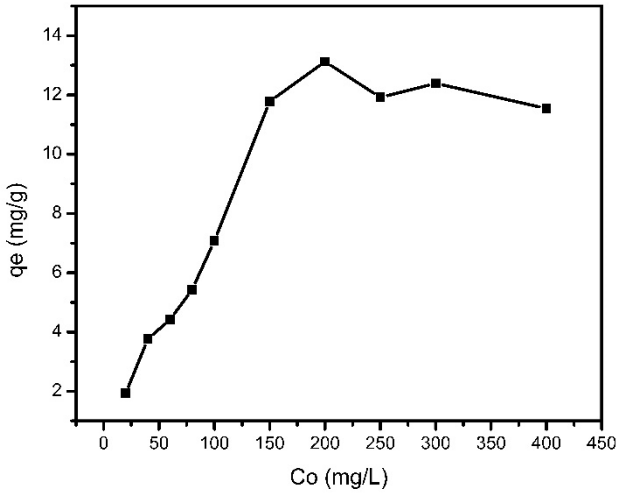

Fig. 5. Effect C_0 on qe and percent removal (C_0: 100-1000 mg/L; pH = 2; T = 25°C; V= 10 mL; m = 0,1 g; agitation speed= 100 rpm; t = 60 minute; particle size= 36µm).

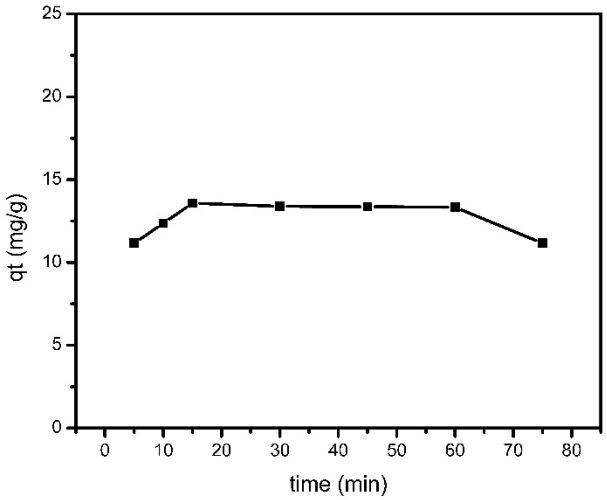

Fig. 6. Influence of contact time on the adsorption of IC dye by CHW (C_0: 200 mg/ L; pH = 2; T = 25 °C; V= 10 mL; m = 0,1 g; agitation speed= 100rpm; t = 15- 75 minute; particle size= 36µm).

dyes requires determining the initial concentration of the biosorption process. Figure 5 shows that the biosorbent's highest adsorption capacity is at a concentration of 200 mg/L, where the value is 13.57 mg/g. The adsorption capacity falls as the starting concentration rises. This results from the biosorbent's active side becoming saturated and dyestuffs competing to interact with the active site. Another study on the adsorption of IC dye by Cinnamon bark (Güler et al., 2021) and *Terminalia catappa* shell (Hevira et al., 2020) revealed the same outcome.

The initial concentration of the dye affects how closely the dye molecule interacts with the surface-active side of the adsorbent (Mushtaq et al., 2016). Alternatively, the driving force or mobility of the dye molecules to diffuse will expand as the initial concentration of the dye increases. The mass change increases the adsorption capacity from dye solution to biosorbent (Sen et al., 2011).

Adsorption capacity depends on how long the biosorbent and adsorbate are in contact before there is a chance of either physical or chemical biosorption. The high adsorption capacity lasts for 5 to 75 minutes, according to the research that has been done (Figure 6). The adsorption

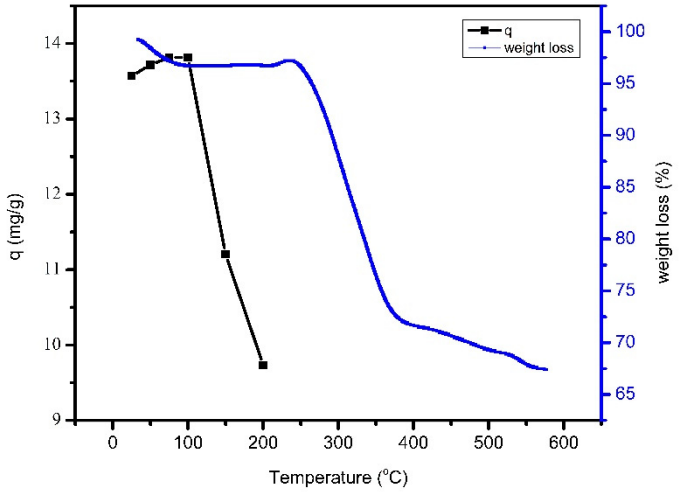

Fig. 7. Relationship between CHW heating temperature and TGA Analysis

capacity peaked at 11.16 mg/g in the first five minutes, increased in the fifteenth minute at 13.57 mg/g, remained constant until the sixty-fifth minute, and then fell in the seventy-fifth minute, as a result of the continuing collision, the dye's continuing release from the adsorbent's active side.

The initial increase in adsorption capacity was due to the presence of pores in the CHW by the BET analysis that had been carried out previously. The surface of the adsorbent saturated with acid will make it positive, thus encouraging the adsorption of IC dye from the solution (Hevira et al., 2020). The biosorption slowed after 60 minutes, and the IC dye molecules started resisting the adsorbent surface as the CHW pores saturated. When this happens, more amounts of indigo carmine are no longer adsorbed (Gupta et al., 2022; Sulistiyo et al., 2020). This phenomenon has been explained by Kubra et al (2021) in crystal violet dye removal using graham flour (Kubra et al., 2021).

The biosorbent's capacity for adsorption is impacted by how hot it is heated. 25–200 °C has been utilized to heat CHW on IC dye adsorption. Figure 7 demonstrates that the optimal temperature for IC dye adsorption by CHW was 25 °C, with an adsorption capacity of 13.57 mg/g. The increase of 13.81 mg/g was attained by heating CHW to a temperature between 75 and 100 °C. This finding proposes an exothermic adsorption mechanism, which thermodynamic studies ultimately validated. The biosorbent is denaturized as the heating temperature rises, which reduces CHW's ability to adsorb IC dye.

The weight loss of the adsorbent over time as the temperature change was calculated using the thermogravimetric method and is crucial for proving the biosorbent's usefulness in densely packed industrial columns that could contain hot zones. The mass losses may be caused by disintegration, gas-solid reaction (oxidation/reduction), or physical or chemical changes (Abderrahim et al., 2015; Seenivasan & Panda, 2017). CHW loses up to 96.84% of its mass at 247 °C. At 378 °C, it drops sharply to 72.24%. The evaporation of water is the first source of weight loss in reaction to a rise in temperature, followed by the degradation of cellulose. TGA provides information on the mechanism and kinetics of the adsorbent's response to temperature variations. Cellulose and hemicellulose disintegrate between 250 and 350 °C, whereas lignin decomposes at temperatures above 350 °C (Huang, 2012).

The adsorption isotherm model was used to explain and predict how a material's adsorption rate depends on the material's concentration in the gas or liquid phase. The adsorption isotherm model was usually used to understand the adsorption mechanism, compare the adsorption performance of various adsorbent materials, and select the optimal adsorbent material for a

particular application (Bazan & Robert, 2023; Yeo et al., 2023). The initial concentration of the dye affects which isotherm model was most appropriate for the actual adsorption procedure. The collected data were tested using the Langmuir, Freundlich, Temkin, and Dubinin-Radushkevich adsorption isotherm models. The total amount of concentration effect numbers was used in the equation. The derived coefficient of determination (R^2) value was considered more acceptable for the isotherm model if it is near one.

Figure 8 and Table 3 suggest that the R^2 value of the isotherm is close to one, indicating that the adsorption meets the Langmuir isotherm model. The Langmuir isotherm model suggests that adsorption proceeds as a uniform, single-layer process of overall active sites (Yeo et al., 2023). Figure 8 d shows that the Dubinin-Radushkevich model has a poor coefficient of determination; Therefore, this model is not suitable for describing the adsorption that occurs. This model assumes a multilayer structure involving Van der Waals forces, has applications for physical adsorption processes, and is a fundamental equation that qualitatively describes the adsorption of gases and vapors on solid sorbents. In contrast, the current research focuses on the adsorption of liquids in solid sorbents (Ayawei et al., 2017). A low coefficient of determination

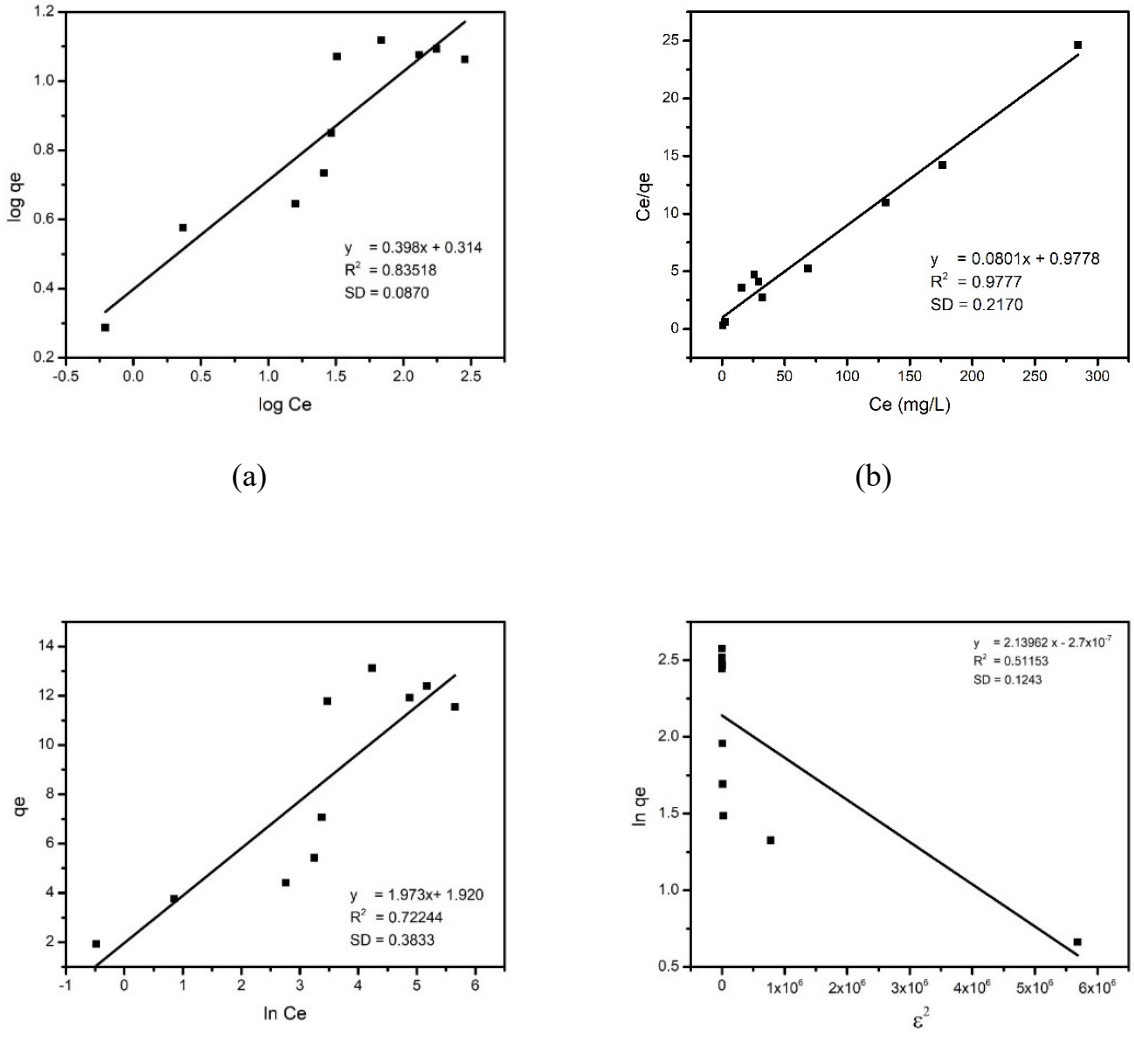

Fig. 8. Freundlich (a), Langmuir (b), Temkin (c), and Dubinin-Radushkevich (d) isotherm plots for the IC dye adsorption.

Table 3. The CHW isotherm parameter for IC dye adsorption.

Parameters	Freundlich	Langmuir	Temkin	Dubinin-Radushkevich
K_F ((L/mg)$^{1/n}$)	2.5015	-	-	-
1/n	0.3149	-	-	-
q_m (mg /g)	-	12.4844	-	1.00
K_L (L/mg)	-	12.2085	-	-
R_L	-	0.0004	-	-
β (J /mol)	-	-	1.973	-
K_T (L /g)	-	-	2.6462	-
K (mol^2 /J^2)	-	-	-	2.1396
E_{DR} (kJ/mol)	-	-	-	1.3673
R^2	0.8352	0.9777	0.7224	0.5115
SD	0.0870	0.2170	0.3833	0.1243

was also recorded when IC dye was adsorbed by *Terminalia Catappa* shell (Hevira et al., 2020) and by cinnamon bark (Güler et al., 2021).

The adsorption mechanism of the adsorbate on the biosorbent was identified using the adsorption kinetics model. The physical and chemical characteristics of the adsorbent and the mass transfer rate during the operation are crucial factors in defining the adsorption mechanism. In this case, the kinetic model is examined using contact time data. The physical and chemical characteristics of the adsorbent and the mass transfer rate process are crucial factors in determining the adsorption mechanism. This study used the pseudo-second-order kinetics model to examine the adsorption mechanism (Güler et al., 2021).

The kinetic of IC dye uptake onto CHW can be shown from Figure 9 and Table 4 that the pseudo-second-order kinetic model is more appropriate for treating IC dye adsorption by CHW with a coefficient of determination (R^2) near 1. The second-order pseudo-reaction model states that the reaction rate depends on the square of the concentration of the reaction products (Hevira et al., 2020), and several processes were implicated in the adsorption mechanism, but the potential rate-controlling step was film diffusion (Ghosh et al., 2020).

The spontaneity of the adsorption process is determined through adsorption thermodynamic studies. The standard Gibbs free energy, enthalpy, and entropy were calculated using the adsorption temperature variation data.

When determining whether an adsorption process occurs spontaneously, the Gibbs free energy (ΔG°) was used. A negative value denotes spontaneous adsorption, while a positive value denotes non-spontaneous adsorption. Whether the adsorption process was endothermic or exothermic was expressed by the enthalpy (ΔH°). When the enthalpy value is negative, adsorption occurs exothermically or releases energy; adsorption adsorbs energy when the enthalpy value is positive. Entropy (ΔS°) expresses the degree of randomness or orderliness in the adsorption reaction. Uncertainty or disorder was reduced if the value was negative and increased if the value was positive (Patil et al., 2020). Table 5 shows that the reaction happens spontaneously and does not require energy or heat.

The potential biosorption mechanism of IC dye onto CHW is based on the many analyses performed during the study. After being exposed to IR before and after biosorption, FTIR showed a change in the stretching and bending vibrations. This result proved that functional groups played a role in the adoption process (Ahmad & Ansari, 2020). The CHW optimization, modeling, and physicochemical characterization research shed light on the IC dye adsorption mechanism. The SEM pictures on the porous and hollow surface of CHW revealed pore-filling IC dye molecules. The adsorption mechanism of IC dye on CHW based on the preceding discussion is shown in Figure 11.

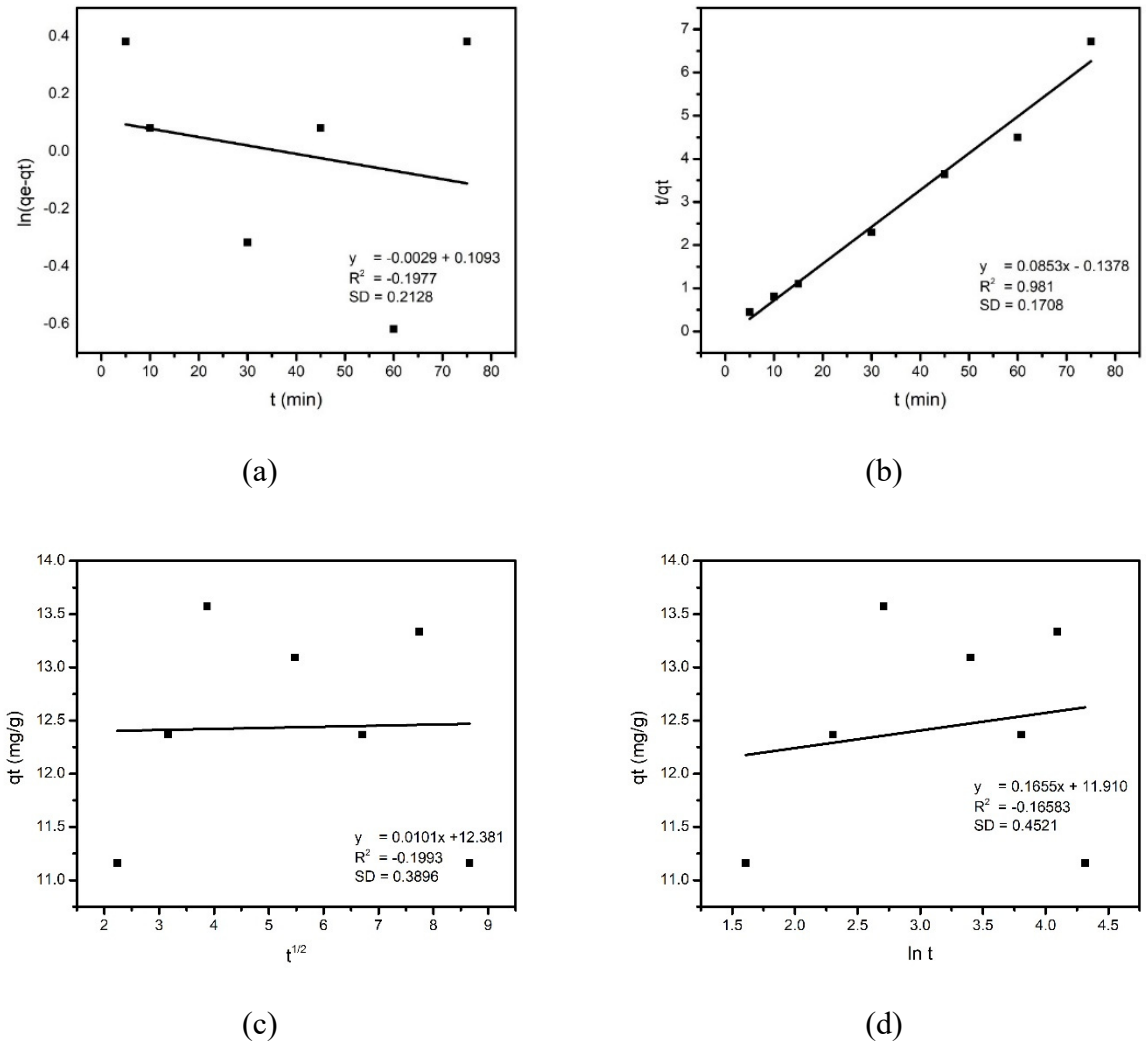

Fig. 9. (a-d) The kinetic of IC dye uptake onto CHW by pseudo-first-order (a), pseudo-second-order (b), intraparticle diffusion (c), and Elovich (d).

Table 4. CHW adsorption IC dye kinetics parameter

Kinetic model	Pseudo-first-order	Pseudo-second-order	Intraparticle Diffusion	Elovich
k_1 (/min)	0.0071	-	-	-
k_2 (g/mg min)	-	-0.0211	-	-
qe (calc) (mg /g)	0.5847	11.1607	-	-
K_{diff} (mg/ g $min^{1/2}$)	-	-	0.0101	-
C (mg/g)	-	-	12.381	-
β (g /mg)	-	-	-	6.0423
α (mg min/g)	-	-	-	2.97 x10^{30}
R^2	-0.1977	0.981	-0.1993	-0.1658
SD	0.2128	0.1708	0.3896	0.4521

As the IC dye structure shows, two of the compound's SO^- points are electrostatically negative. Furthermore, CHW had a net positive surface charge below the pHpzc. Chemisorption is an irreversible process where adsorbate is adsorbed to the surface of the functional adsorbent through electrostatic attractions. **Kinetic studies on chemically mediated IC uptake caused**

Table 5. Thermodynamic data on the adsorption of IC dye on CHW

Parameter	Temperature (K)			Result
	298	308	318	
ΔG° (kJ mol^{-1})	-2.2329	-2.2963	-1.9211	Spontaneous
ΔH° (kJ mol^{-1})		-6.9517		Exothermic
ΔS° (kJ mol^{-1} K^{-1})		0.0156		disorder decreases

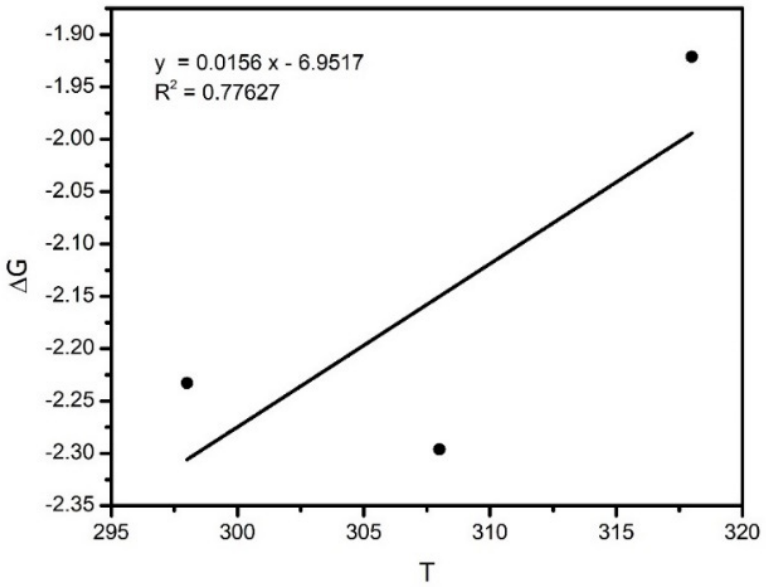

Fig. 10. Adsorption thermodynamics graphs for IC dye on CHW at 298, 308, and 318 K.

by electrostatic chemical interactions between negatively charged substances of IC and the biosorbent surface's positive charge are responsible for absorption (Tran et al., 2017). This phenomenon was also shown in a study by Kabir et al. (2022) on the absorption of metal anions using tea waste (Kabir et al., 2021).

The maximum adsorption capacity of CHW on IC dye was higher than that of activated carbon made from the bark of *Swietenia mahagoni* on methyl orange dye and reactive red 120 dye, which was 6,071 mg/g (Ghosh et al., 2020) and 5,402 mg/g (Chakraborty et al., 2021) respectively. These hues were all anionic hues as well. The following compares various biosorbents for adsorbing IC dye from solutions with variations in adsorption.

The effectiveness of IC dye adsorption and the reusability of CHW were investigated using the adsorption-desorption process. Reusability was essential in assessing the economic and environmental effects of biosorbents (Kubra, Salman, & Hasan, 2021; Sharma et al., 2018). Regeneration eliminates the need for adsorbent and lowers adsorption costs. The cycles of IC dye adsorption and desorption by CHW were evaluated using NaOH, shown in Figure 12.

Another literature (Szygula et al., 2008) reported that anionic dyes could be desorbed using NaOH, which is faster than other bases. At high alkaline pH, the negatively charged sites on the biosorbent encourage the decay of the anionic dyes as a result of electrostatic repulsion. Under high pH conditions, the negatively charged sites on the biosorbent will encourage the decay of anionic dyes due to electrostatic repulsion (Mahmoodi et al., 2011).

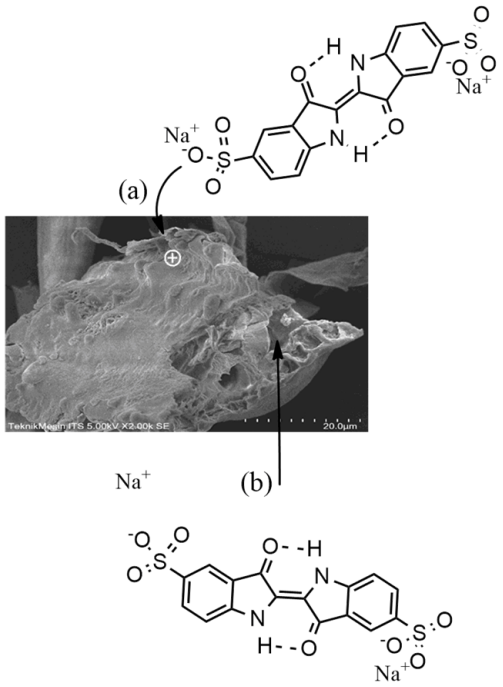

Fig. 11. Prediction of the mechanism of indigo carmine dye adsorption on CHW (a) electrostatic interaction, and (b) pore-filling

Table 6. Comparison of the Indigo carmine dye's ability to bind to different biosorbents

Biosorbent	T (K)	pH	qe (mg/g)	References
Bazil nut shells	303	5	1.09	(de Oliveira Brito et al., 2010)
Terminalia catappa shells	298	2	26.77	(Hevira et al., 2020)
Cinnamon bark	298	2	3.00	(Güler et al., 2021)
Corn husk waste	298	2	13.57	This study
Activated pomegranate peel	298	2	158.73	(Abbas et al., 2022)

Less IC dye could be adsorbed with more cycles since the CHW surface's active site became filled. When the pH was too high, CHW started to deteriorate and clog the surface's pores and functional areas. The adsorption capacity has diminished due to the strong interactions between IC dye and several active sites with higher binding energies(Hevira et al., 2020). High reuse of CHW due to its capacity to adsorb IC dye for five cycles with high removal of> 80%.

The Environmental Chemistry Laboratory at Andalas University provided the laboratory wastewater used in the experiment in August 2022. The best adsorption conditions are used to treat laboratory wastewater in a small-scale setting. In 15 minutes of stirring at 100 rpm, the IC dye removal was used with 0.1 g of CHW with a particle size of less than 36 µm. The adsorption technique was conducted to compare the adsorption capacity under two different circumstances (optimum pH and natural solution pH). With a removal efficiency of 32.10% at natural pH (without pH correction), Table 7 shows that CHW performed well for IC dye adsorption in wastewater. Elimination effectiveness was 89.1% at the optimal biosorption pH of 2. The efficiency of CHW as a cheap biosorbent is therefore confirmed.

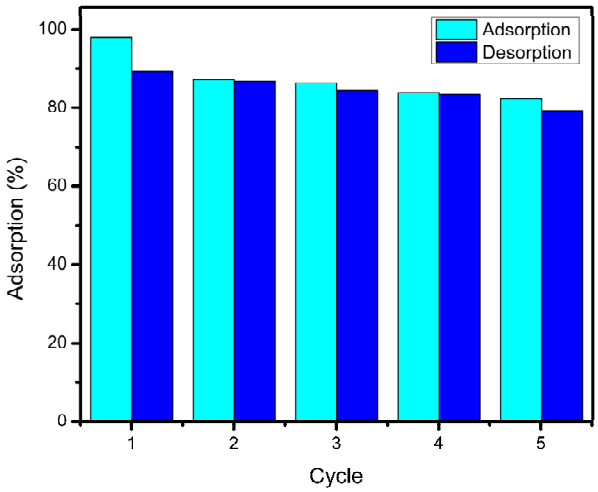

Fig. 12. The IC dye cycle of CHW adsorption and desorption

Table 7. Comparison of CHW efficacy for IC dye adsorption

Wastewater condition	pH	Contact time (min)	C_0 (mg/L)	C_e (mg/L)	% Removal
Optimum	2	15	4.7487	0.5217	89.01
Real	7.505	15	4.9661	3.3720	32.10

CONCLUSIONS

The complete adsorption study of indigo carmine dye by acid-activated CHW from an aqueous solution was investigated. The simple activated method using 0.01M HNO3 reveals the maximum capacity for removal of IC at pH 2, initial IC dye values of 200 mg/L, and contact time of 15 minutes, leading to a maximum adsorption capacity of 13.57 mg/g in 25 °C temperature. For adsorption, the Langmuir isotherm model and the pseudo-second-order kinetic model are both valid (R2 = 0.981 and 0.977, respectively). The adsorption process is exothermic and spontaneous and causes less disarray, as thermodynamic characteristics indicate (S° = 0.0077 kJ/mol K). Recycling CHW is simple (five times). In a real environment, the pH level of 2 allowed the removal of 89.01 per cent of the original effluent. Finally, it has been demonstrated that CHW is an effective, low-cost adsorbent for IC dye that is also quick, natural, affordable, and accessible.

ACKNOWLEDGEMENTS

The author would like to thank the Department of Chemistry, Andalas University, for the laboratory facilities and reviewers for their valuable comments.

GRANT SUPPORT DETAILS

We would like to thank the Ministry of Finance of the Republic of Indonesia for supporting this research through the Education Fund Management Agency (No. KET-259/LPDP.4/2021), award number: 20201221685770

CONFLICT OF INTEREST

The authors declare to have no competing interests to declare that are relevant to the content of this article.

LIFE SCIENCE REPORTING

No life science threat was practised in this research

DATA AVAILABILITY

The datasets generated during and analyzed during the current study are available from the corresponding author on reasonable request

REFERENCES

Abbas, M., Harrache, Z., Aksil, T., & Trari, M. (2022). Removal of indigo carmine (IC) in aqueous solution onto activated pomegranate peel (APP) by adsorption process: Kinetic and thermodynamic studies. *Journal of Engineered Fibers and Fabrics*, *17*(Ic). https://doi.org/10.1177/15589250211018195

Abderrahim, B., Abderrahman, E., Mohamed, A., Fatima, T., Abdesselam, T., & Krim, O. (2015). Kinetic Thermal Degradation of Cellulose, Polybutylene Succinate and a Green Composite: Comparative Study. *World Journal of Environmental Engineering, Vol. 3, 2015, Pages 95-110*, *3*(4), 95–110. https://doi.org/10.12691/WJEE-3-4-1

Ahmad, R., & Ansari, K. (2020). Polyacrylamide-Grafted Actinidia deliciosa peels powder (PGADP) for the sequestration of crystal violet dye: isotherms, kinetics and thermodynamic studies. *Applied Water Science*, *10*(8), 1–15. https://doi.org/10.1007/s13201-020-01263-7

Al-Abbad, E., & Alakhras, F. (2020). Removal of dye acid red 1 from aqueous solutions using chitosan-iso-vanillin sorbent material. *Indonesian Journal of Science and Technology*, *5*(3), 352–365. https://doi.org/10.17509/ijost.v5i3.24986

Alamrani, N. A., & Al-Aoh, H. A. (2021). Elimination of Congo Red Dye from Industrial Wastewater Using Teucrium polium L. as a Low-Cost Local Adsorbent. *Adsorption Science and Technology*, *2021*. https://doi.org/10.1155/2021/5728696

Amer, H., El-Gendy, A., & El-Haggar, S. (2017). Removal of lead (II) from aqueous solutions using rice straw. *Water Science and Technology*, *76*(5), 1011–1021. https://doi.org/10.2166/wst.2017.249

Ayawei, N., Ebelegi, A. N., & Wankasi, D. (2017). Modelling and Interpretation of Adsorption Isotherms. *Journal of Chemistry*, *2017*, 1–11. https://doi.org/10.1155/2017/3039817

Bazan, A., & Robert, W. (2023). Adsorption of cationic dye on nanostructured biocarbons : kinetic and thermodynamic study. *Applied Nanoscience*, *0123456789*. https://doi.org/10.1007/s13204-023-02775-9

Chakraborty, T. K., Ghosh, G. C., Akter, M. N., Audhikary, K., Islam, M. S., Ghosh, P., Zaman, S., Habib, A., & Kabir, A. H. M. E. (2021). Biosorption of Reactive Red 120 Dye from Aqueous Solutions by using Mahagoni (Swietenia mahagoni) Wood and Bark Charcoal: Equilibrium, and Kinetic Studies. *Pollution*, *7*(4), 905–921. https://doi.org/10.22059/POLL.2021.325135.1110

Chandra, P. P., Visakoti, V., & Naidu, D. A. (2019). Studies on Biosorption of Alizarin Red dye using Prawn Shell Waste Powder. *International Research Journal of Engineering and Technology (IRJET)*, *06*(02).

de Oliveira Brito, S. M., Andrade, H. M. C., Soares, L. F., & de Azevedo, R. P. (2010). Brazil nut shells as a new biosorbent to remove methylene blue and indigo carmine from aqueous solutions. *Journal of Hazardous Materials*, *174*(1–3), 84–92. https://doi.org/10.1016/j.jhazmat.2009.09.020

Ferreira, R. M., de Oliveira, N. M., Lima, L. L. S., Campista, A. L. D. M., & Stapelfeldt, D. M. A. (2019). Adsorption of indigo carmine on Pistia stratiotes dry biomass chemically modified. *Environmental Science and Pollution Research*, *26*(28), 28614–28621. https://doi.org/10.1007/s11356-018-3752-x

Ghosh, G. C., Chakraborty, T. K., Zaman, S., Nahar, M. N., & Kabir, A. H. M. E. (2020). Removal

of methyl orange dye from aqueous solution by a low-cost activated carbon prepared from mahagoni (Swietenia mahagoni) Bark. *Pollution*, *6*(1), 171–184. https://doi.org/10.22059/POLL.2019.289061.679

Güler, M., Çetintaş, S., & Bingöl, D. (2021). Cinnamon bark as low-cost and eco-friendly adsorbent for the removal of indigo carmine and malachite green dyestuffs. *International Journal of Environmental Analytical Chemistry*, *101*(6), 735–757. https://doi.org/10.1080/03067319.2019.1670171

Gupta, T., Ansari, K., Lataye, D., Kadu, M., Khan, M. A., Mubarak, N. M., Garg, R., & Karri, R. R. (2022). Adsorption of Indigo Carmine Dye by Acacia nilotica sawdust activated carbon in fixed bed column. *Scientific Reports*, *12*(1), 1–14. https://doi.org/10.1038/s41598-022-19595-6

Hasan, M. M., Shenashen, M. A., Hasan, M. N., Znad, H., Salman, M. S., & Awual, M. R. (2021). Natural biodegradable polymeric bioadsorbents for efficient cationic dye encapsulation from wastewater. *Journal of Molecular Liquids*, *323*, 114587. https://doi.org/10.1016/j.molliq.2020.114587

Hevira, L., Zilfa, Z., Rahmayeni, R., Ighalo, J. O., & Zein, R. (2020). Biosorption of indigo carmine from aqueous solution by Terminalia Catappa shell. *Journal of Environmental Chemical Engineering*, *8*(5), 1–11. https://doi.org/10.1016/j.jece.2020.104290

Hoang, M. T., Pham, T. D., Pham, T. T., Nguyen, M. K., Nu, D. T. T., Nguyen, T. H., Bartling, S., & Van der Bruggen, B. (2021). Esterification of sugarcane bagasse by citric acid for Pb2+ adsorption: effect of different chemical pretreatment methods. *Environmental Science and Pollution Research*, *28*(10), 11869–11881. https://doi.org/10.1007/s11356-020-07623-9

Huang, F. Y. (2012). Thermal properties and thermal degradation of cellulose tri-stearate (CTs). *Polymers*, *4*(2), 1012–1024. https://doi.org/10.3390/polym4021012

Hwa, S., Huey, C., Islam, A., Abdulkareem-alsultan, G., Joseph, C. G., Janaun, J., Hin, Y., Khandaker, S., Jahirul, G., Znad, H., & Awual, R. (2022). *Sustainable toxic dyes removal with advanced materials for clean water production : A comprehensive review*. *332*(December 2021). https://doi.org/10.1016/j.jclepro.2021.130039

Islam, A., Hwa, S., Taufiq-yap, Y. H., Huey, C., Vo, D. N., Lokman, M., Hasan, M., Khan, M. A. R., Nur, A. S. M., & Awual, R. (2021). Resources , Conservation & Recycling Step towards the sustainable toxic dyes removal and recycling from aqueous solution- A comprehensive review. *Resources, Conservation & Recycling*, *175*(May), 105849. https://doi.org/10.1016/j.resconrec.2021.105849

Kabir, M. M., Mouna, S. S. P., Akter, S., Khandaker, S., Mohammed, N., Mohinuzzaman, M., Islam, A., & Shenashen, M. A. (2021). Tea waste based natural adsorbent for toxic pollutant removal from waste samples. *Journal of Molecular Liquids*, *322*, 115012. https://doi.org/10.1016/j.molliq.2020.115012

Kubra, K. T., Salman, M. S., & Hasan, M. N. (2021). Enhanced toxic dye removal from wastewater using biodegradable polymeric natural adsorbent. *Journal of Molecular Liquids*, *328*, 115468. https://doi.org/10.1016/j.molliq.2021.115468

Kubra, K. T., Salman, M. S., Znad, H., & Hasan, M. N. (2021). Efficient encapsulation of toxic dye from wastewater using biodegradable polymeric adsorbent. *Journal of Molecular Liquids*, *329*, 115541. https://doi.org/10.1016/j.molliq.2021.115541

Lagergren, S. (1898). *About the theory of so-called adsorption of soluble substances* (24(4)). Kungliga Svenska Vetenskapsademiens Handlingar.

Lakshmi, U. R., Srivastava, V. C., Mall, I. D., & Lataye, D. H. (2009). Rice husk ash as an effective adsorbent: Evaluation of adsorptive characteristics for Indigo Carmine dye. *Journal of Environmental Management*, *90*(2), 710–720. https://doi.org/10.1016/j.jenvman.2008.01.002

Mahmoodi, N. M., Arami, M., Bahrami, H., & Khorramfar, S. (2011). The Effect of pH on the Removal of Anionic Dyes from Colored Textile Wastewater Using a Biosorbent. *Journal of Applied Polymer Science*, *120*, 2996–3003. https://doi.org/10.1002/app.33406

Malik, D. S., Jain, C. K., Yadav, A. K., Kothari, R., & Pathak, V. V. (2016). *Removal of methylene blue dye in aqueous solution by agricultural waste*. *3*(7), 864–880.

Md. Munjur, H., Hasan, M. N., Awual, M. R., Islam, M. M., Shenashen, M. A., & Iqbal, J. (2020). Biodegradable natural carbohydrate polymeric sustainable adsorbents for efficient toxic dye removal from wastewater. *Journal of Molecular Liquids*, *319*, 114356. https://doi.org/10.1016/j.molliq.2020.114356

Mishra, S., Yadav, S. S., Rawat, S., Singh, J., & Koduru, J. R. (2019). Corn husk derived magnetized activated carbon for the removal of phenol and para-nitrophenol from aqueous solution: Interaction mechanism, insights on adsorbent characteristics, and isothermal, kinetic and thermodynamic properties. *Journal of Environmental Management*, *246*(June), 362–373. https://doi.org/10.1016/j.

jenvman.2019.06.013
Mushtaq, M., Bhatti, H. N., Iqbal, M., & Noreen, S. (2016). Eriobotrya japonica seed biocomposite efficiency for copper adsorption: Isotherms, kinetics, thermodynamic and desorption studies. *Journal of Environmental Management*, *176*, 21–33. https://doi.org/10.1016/j.jenvman.2016.03.013
Paşka, O. M., Pəcurariu, C., & Muntean, S. G. (2014). Kinetic and thermodynamic studies on methylene blue biosorption using corn-husk. *RSC Advances*, *4*(107), 62621–62630. https://doi.org/10.1039/c4ra10504d
Patil, S. A., Kumbhar, P. D., Patil, S. K., Vadiyar, M. M., Suryawanshi, U. P., Jambhale, C. L., Anuse, M. A., Kim, J. H., & Kolekar, S. S. (2020). Dynamic adsorption of toxic indigo carmine dye on bio-inspired synthesised Fe3O4 nanoparticles: kinetic and thermodynamic study. *International Journal of Environmental Analytical Chemistry*, *00*(00), 1–23. https://doi.org/10.1080/03067319.2020.1734197
Paul, G., Murthy, R., & Bengal-, W. (2016). *Studies On Bio-Chemical Thermodynamics Of Lead Biosorption From Aqueous Chemical Thermodynamics Of Lead Biosorption From Aqueous System Using Corn Husk Biomass As Biosorbant Agent*. *8*(09), 3792–3798.
Ponce, J., Andrade, J. G. da S., dos Santos, L. N., Bulla, M. K., Barros, B. C. B., Favaro, S. L., Hioka, N., Caetano, W., & Batistela, V. R. (2021). Alkali pretreated sugarcane bagasse, rice husk and corn husk wastes as lignocellulosic biosorbents for dyes. *Carbohydrate Polymer Technologies and Applications*, *2*(March), 1–8. https://doi.org/10.1016/j.carpta.2021.100061
Purnaningtyas, M. A. K., Sudiono, S., & Siswanta, D. (2020). Synthesis of activated carbon/chitosan/alginate beads powder as an adsorbent for methylene blue and methyl violet 2b dyes. *Indonesian Journal of Chemistry*, *20*(5), 1119–1130. https://doi.org/10.22146/ijc.49026
Rahman, A. K. M. L., Sarker, A., Ahmed, N., Mustofa, M., & Awal, A. (2021). Efficient removal of toxic textile dye using petiole part (stem) of nymphaea alba. *Pollution*, *7*(3), 643–656. https://doi.org/10.22059/POLL.2021.314204.943
Ramadhani, P., Chaidir, Z., Zilfa, Z., Fauzia, S., & Zein, R. (2021). Isolation of chitosan from shrimp shell (Metapenaeus monoceros) as adsorbent for removal of metanil yellow dyes. *Journal of the Iranian Chemical Society*, 1–15. https://doi.org/10.1007/s13738-021-02385-8
Sanka, P. M., Rwiza, M. J., & Mtei, K. M. (2020). Removal of Selected Heavy Metal Ions from Industrial Wastewater Using Rice and Corn Husk Biochar. *Water, Air, and Soil Pollution*, *231*(5), 1–13. https://doi.org/10.1007/s11270-020-04624-9
Seenivasan, A., & Panda, T. (2017). Protein Characterization by Thermal Property Measurement. *Glass Transition and Phase Transitions in Food and Biological Materials*, *Cd*, 305–391. https://doi.org/10.1002/9781118935682.ch14
Sen, T. K., Afroze, S., & Ang, H. M. (2011). Equilibrium, kinetics and mechanism of removal of methylene blue from aqueous solution by adsorption onto pine cone biomass of Pinus radiata. *Water, Air, and Soil Pollution*, *218*(1–4), 499–515. https://doi.org/10.1007/s11270-010-0663-y
Sengupta, P., & Balomajumder, P. (2014). Potential of Corn Husk Leaves for the Co-Removal of Phenol and Cyanide From Waste Water Using Simultaneous Adsorption and Biodegradation. *International Journal of Research in Engineering and Technology*, *03*(02), 700–707. https://doi.org/10.15623/ijret.2014.0302124
Shan, W., Zhao, Z., Fang, D., Lou, Z., Xu, J., Yue, S., Biswas, B. K., & Xiong, Y. (2013). Investigation on the selective adsorption of Mo(VI) by using modified rice husk and corn straw. *Waste and Biomass Valorization*, *4*(2), 385–393. https://doi.org/10.1007/s12649-012-9149-z
Sharma, S., Hasan, A., Kumar, N., & Pandey, L. M. (2018). Removal of methylene blue dye from aqueous solution using immobilized Agrobacterium fabrum biomass along with iron oxide nanoparticles as biosorbent. *Environmental Science and Pollution Research*, *25*(22), 21605–21615. https://doi.org/10.1007/s11356-018-2280-z
Sulistiyo, Y. A., Rofi'ah, F., Suwardiyanto, Nugraha, A. S., Zulfikar, & Sunnardianto, G. K. (2020). Isothermal and kinetic adsorption of anionic dye onto impregnated silica gels with aluminum. *Environmental Engineering and Management Journal*, *19*(8), 1299–1308. https://doi.org/10.30638/eemj.2020.123
Szygula, A., Ruiz, M., Guibal, E., & Sastre, A. M. (2008). Removal of an Anionic Reactive Dye by Chitosan and its Regeneration. *Energy And Environmental Engineering Series*, *1*, 24–30. http://gateway.isiknowledge.com/gateway/Gateway.cgi?GWVersion=2&SrcAuth=AegeanSoftware&SrcApp=NoteExpress&DestLinkType=FullRecord&DestApp=WOS&KeyUT=000262931000005

Tran, H. N., You, S. J., Hosseini-Bandegharaei, A., & Chao, H. P. (2017). Mistakes and inconsistencies regarding adsorption of contaminants from aqueous solutions: A critical review. *Water Research*, *120*, 88–116. https://doi.org/10.1016/j.watres.2017.04.014

Yeo, J. Y. J., Khaerudini, D. S., Soetaredjo, F. E., Waworuntu, G. L., Ismadji, S., Putranto, A., & Sunarso, J. (2023). Experimental and modelling study of adsorption isotherms of amoxicillin, ampicillin and doripenem on bentonite-chitosan composite. *South African Journal of Chemical Engineering*, *43*(October 2022), 38–45. https://doi.org/10.1016/j.sajce.2022.09.013

Yous, R., Cherifi, H., & Khalladi, R. (2019). Comparative mass transfer study of basic and acid magenta adsorption onto natural clay. *Indonesian Journal of Chemistry*, *19*(4), 1031–1042. https://doi.org/10.22146/ijc.41820

Zein, R., Purnomo, J. S., Ramadhani, P., Alif, M. F., & Safni, S. (2022). Lemongrass (Cymbopogon nardus) leaves biowaste as an effective and low-cost adsorbent for methylene blue dyes removal: isotherms, kinetics, and thermodynamics studies. *Separation Science and Technology (Philadelphia)*, *00*(00), 1–17. https://doi.org/10.1080/01496395.2022.2058549